POLITECNICO DI TORINO
Repository ISTITUZIONALE

Development of In–Cu binary oxide catalysts for hydrogenating CO2 via thermocatalytic and electrocatalytic routes

Original
Development of In–Cu binary oxide catalysts for hydrogenating CO2 via thermocatalytic and electrocatalytic routes / Mezzapesa, M.P., Salomone, F., Guzmán, H., Zammillo, F., Millini, R., Bua, L., Marra, G., Tacca, A., Marrazzo, R., Russo, N., Pirone, R., Hernandez, S., Bensaid, S.. - In: INORGANIC CHEMISTRY FRONTIERS. - ISSN 2052-1553. - ELETTRONICO. - 11:(2024), pp. 2319-2338. [10.1039/d3qi02499g]

Availability:
This version is available at: 11583/2988113 since: 2024-07-22T18:29:43Z

Publisher:
Royal Society of Chemistry - RSC

Published
DOI:10.1039/d3qi02499g

Terms of use:

This article is made available under terms and conditions as specified in the corresponding bibliographic description in the repository

Publisher copyright

(Article begins on next page)

27 June 2026

International Journal of Pharmaceutics 657 (2024) 124148

Contents lists available at ScienceDirect

International Journal of Pharmaceutics

journal homepage: www.elsevier.com/locate/ijpharm

Evaluation of layer-by-layer assembly systems for drug delivery and antimicrobial properties in orthopaedic application

Parinaz Mofazali [a], Masoud Atapour [a,*], Miho Nakamura [b], Manuela Galati [c], Abdollah Saboori [c]

[a] Department of Materials Engineering, Isfahan University of Technology, Isfahan 84156-83111, Iran
[b] Medicity Research Laboratory, Faculty of Medicine, University of Turku Tykistökatu 6, 20520 Turku, Finland
[c] Integrated Additive Manufacturing Center (IAM), Department of Management and Production Engineering, Politecnico di Torino, Corso Duca Degli Abruzzi 24, 10129 Torino, Italy

ARTICLE INFO

Keywords:
Electron beam melting
Layer-by-layer self-assembly
Polymeric carriers
Drug release
Insulin-like growth factor-1
Cefazolin

ABSTRACT

Layer-by-layer self-assembly systems were developed using monolayer and multilayer carriers to prevent infections and improve bone regeneration of porous Ti-6Al-4V scaffolds. These polymeric carriers incorporated (Gel/Alg-IGF-1 + Chi-Cef) and (4Gel/Alg-IGF-1 + Chi-Cef) on the surface of porous implants produced via electron beam melting (EBM). The results showed that the drug release from multilayer carriers was higher than that of monolayers after 14 days. However, the carrier containing Gel/Alg-IGF-1 + Chi-Cef exhibited more sustained behavior. Cell morphology was characterized, revealing that multilayer carriers had higher cell adhesion than monolayers. Additionally, cell differentiation was significantly greater for (Gel/Alg-IGF-1) + Chi-Cef, and (4Gel/Alg-IGF-1) + Chi-Cef multilayer carriers than for the monolayer groups after 7 days. Notably, the drug dosage was effective and did not interfere, and the cell viability assay showed safe results. Antibacterial evaluations demonstrated that both multilayer carriers had a greater effect on Staphylococcus aureus during treatment. The carriers containing lower alginate had notably less effect than the other studied carriers. This study aimed to test systems for controlling drug release, which will be applied to improve MG63 cell behavior and prevent bacterial accumulation during orthopaedic applications.

1. Introduction

Ti6Al4V (Ti64) implants are widely used to treat one disease. However, bacterial colonization and interaction with cells pose a significant challenge to their constant use (Pina et al., 2019). The surface of an implant is susceptible to bacterial infections, mostly due to the development of a biofilm on its surface. This can result in a weakened immune response at the implant/tissue interface (Oliva et al., 2021). To address this issue, a wide range of antibacterial coatings for bone implants has been developed (Oliveira et al., 2018). The biocompatibility of titanium implants can be correlated with a surface protein layer that is produced under physiological conditions. This layer shields adhering bacteria from the human immune system and bactericidal medicines via a variety of mechanisms, once a biofilm has formed (Donlan and Costerton, 2002; Dunne, 2002; Harris and Richards, 2006).

The riskiest time for infection is immediately following implantation since the implant's host immunity capacity is impaired. Several strategies, including strict aseptic surgical protocols, have been suggested to reduce bacterial contamination. However, evidence suggests that bacterial invasion typically happens after surgery (Arciola et al., 2018). To prevent postoperative infection, individuals receiving implantation regularly receive systemic antibiotics (Moris et al., 2023; Roca-Millan et al., 2021). However, the use of systemic antibiotics has significant drawbacks, including potential toxicity and limited drug delivery to the target site. Antibiotic topical treatment has so garnered a lot of interest among researchers (Dallo et al., 2023; Eady and Cove, 1990). In fact, they are working to create coatings for titanium implants that are loaded with antibiotics (Gallo et al., 2014; Stigter et al., 2002; Yu et al., 2015), such as carbenicillin, amoxicillin, cephazolin, tobramycin, and vancomycin (Chen et al., 2023). On titanium implants, antibiotics have been infused into the porous hydroxyapatite coating (Engesaeter et al., 2003). The physical absorption of these drugs onto calcium phosphate surfaces restricts their loaded dose and release characteristics (Fosca et al., 2022). Biodegradable polymer materials are used to create controlled-release antibiotic coatings for titanium implants. Antibiotics are released more slowly than from calcium phosphates (Wall et al., 2021).

* Corresponding author.
E-mail address: m.atapour@cc.iut.ac.ir (M. Atapour).

https://doi.org/10.1016/j.ijpharm.2024.124148
Received 4 January 2024; Received in revised form 2 April 2024; Accepted 21 April 2024
Available online 22 April 2024
0378-5173/© 2024 Elsevier B.V. All rights reserved.

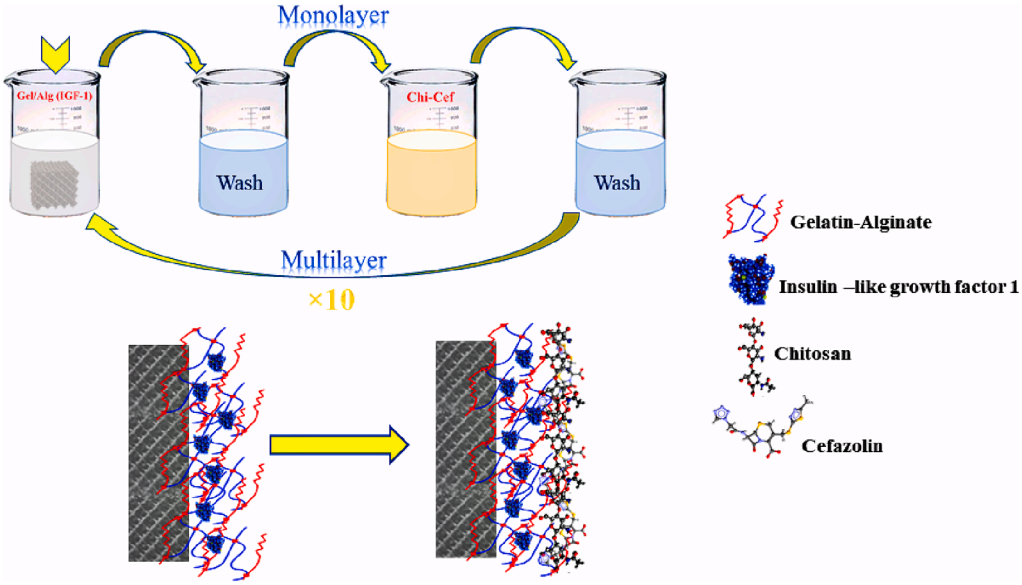

Fig. 1. Schematic of the loading carriers development procedure.

Certain bioactive compounds, such as chitosan, can prevent bacterial adherence and/or cause bacterial death. Chitosan is known for its extraordinary affinity for proteins, as well as its biocompatibility, biodegradability, physiological inertness, and antibacterial and fungistatic properties (Jiménez-Gómez and Cecilia, 2020). In addition, chitosan has been found to induce the differentiation of osteoprogenitor cells (Mathews et al., 2011) and enhance osteoblast cell adhesion (Kjalarsdóttir et al., 2019), viability, alkaline phosphatase activity, and phenotypic expression as various carriers for several active agents (Aranaz et al., 2021). Furthermore, polyelectrolyte multilayers made of chitosan and hyaluronic acid were created on titanium using layer-by-layer (LbL) self-assembly to achieve long-lasting antibacterial ability (Chua et al., 2008). In fact, multilayered polyelectrolyte films can reduce bacterial adherence by approximately 80 % (Kovačević et al., 2016). As a result, chitosan carriers are highly desirable as they can improve the implant capacity for tissue integration and antibacterial defense. The layer-by-layer assembly is a well-known method for applying thin film coatings. It creates a carrier by depositing consecutive layers of materials with opposite charges. The flexibility of this method enables the incorporation of a wide range of materials and capabilities (Matabola et al., 2015). Ziminska et al. demonstrated that for the mechanical support of open-cell structures, it is possible to modify the mechanical characteristics of a porous structure without significantly reducing its porosity by depositing a mechanically strong thin layer (Ziminska et al., 2016). On the other hand, the LbL (Min et al., 2016) was used to simultaneously release active drugs (Li et al., 2022). The LbL process involves cyclic submersion of the surface in polycations and polyanions charged with polyelectrolyte solutions, creating layers on the substrate (Baughman et al., 2002). The layers adhere to each other through numerous interactions between molecules, including hydrophobic bonds and covalent bonding (Xiao et al., 2016). The integration of medicines and growth factors into polyelectrolyte solutions is a crucial aspect. Specifically, the utilization of Ti64 porous scaffolds has addressed the limitations of stress shielding and bioinertness by imparting osteoconductive and antimicrobial properties. In our study, we employed polymeric carriers containing IGF-1 (Insulin-like growth factor 1) and cefazolin for bone regeneration and infection prevention, respectively. These carriers were skillfully designed to incorporate antibiotics into a top layer coating, synergistically combined with IGF-1 within the polymeric matrix. The goal was to enhance both antibacterial properties and osteointegration in both monolayer and multilayer scaffold structures. Notably, prior research on dual release mechanisms in Gyroid lattice scaffolds was conducted by Yavari et al. (Amin Yavari et al., 2020). In our investigation, we explored the influence of the chemical composition ratio of blended anionic polymers and the impact of increasing layers on the encapsulation of IGF-1 and Cefazolin within dode-thin lattice Ti64 scaffolds. Remarkably, the dual release of IGF-1 and Cefazolin has not been previously investigated in any lattice structures.

2. Material and Method

2.1. Scaffold preparation

Cubic-dodethin-shaped Ti64 porous scaffolds with 15 × 15 × 15 mm^3 dimensions were produced using an Arcam A2X EBM machine and used as the base substrate in this study. The surfaces of each sample were etched using a solution of HF, HNO_3, and deionized water (2:3:5) until a suitable surface was achieved. Subsequently, the specimens were washed sequentially in deionized water. Finally, the samples were modified to achieve bioactive properties by alkali heat treatment (Mofazali et al., 2024). The scaffolds were immersed in a 5 M NaOH solution at 60 °C for 24 h. Subsequently, the implants were heated to 600 °C for 1 h at a controlled rate of 5 °C/min.

2.2. Layer-by-Layer assembly (LbL) process and drug loading

In brief, the bone scaffolds underwent the LbL procedure, which involved coating them with multiple layers. The first cycle of coating consisted of dipping the scaffolds in a solution containing IGF-1 (0.02 mg/ml) and an optimum blend of polymer 4Gel/Alg (8:2) or Gel/Alg (5:5), based on the degradation rate (Mofazali et al., 2024). The final dip involved a chitosan solution loaded with cefazolin (0.4 mg/ml). This cycle was repeated up to five times to form monolayer and multilayer coatings, which was the optimum cycle. Dipping cycles were performed to determine the maximum drug with a non-brittle, thin, and non-toxic coating. The scaffolds were then soaked in each solution and incubated for 10 min. Subsequently, the specimens were washed with DI water for 1 min, as shown in Fig. 1.

2.3. Surface and morphology characterization

The morphology and carrier thickness of the specimens were examined using a scanning electron microscope (SEM, Philips XL30,

Netherlands). To acquire representative photos of the coated specimens, several randomly selected regions of the implant surface were examined. The chemical composition and functional chemical group of the coatings were analyzed using Fourier transform infrared (FTIR) spectra obtained with an attenuated total reflectance accessory (ATR) in the 800–2000 cm^{-1} scanning range.

2.4. Nanoindentation test

Nanoindentation measurements were carried out using the constant load and unload mode in a Hysitron Inc. TriboScope nanomechanical test equipped with a 2D transducer and complete software. The indenter used was a Berkovich diamond indenter. To evaluate the bonding strength between substrates and coatings, as well as to analyze adhesion systems an atomic force microscope (AFM) was used (Nanoscope III from Digital Instruments, USA). Hardness and Young's modulus were determined using the Oliver and Pharr method (Oliver and Pharr, 1992).

2.5. Evaluation of cytotoxicity and cell adhesion

Human osteoblast-like MG-63 cells were cultured in DMEM (Gibco, USA) with 10 % fetal bovine serum (FBS) and 1 % penicillin–streptomycin at 37 °C in a 5 % CO_2 humidified atmosphere. The conditioned medium was prepared by soaking the scaffolds in the cell culture medium without FBS for 24 h. Then, the medium was collected and sterilized using a 0.22 um filter. The cells were seeded into 96-well plates at a density of 10^4 cells/well and cultured in the conditioned medium for 1, 3 and 7 days. The WST-8 assay was carried out using commercially available cell-counting kits CCK-8® (Dojindo CK04, Dojindo Laboratories, Kumamoto, Japan), following the supplier's instructions. The relationship between color intensity and cell viability was found to be similar to MTT (Ishiyama et al., 1997). After that, 10 µL of CCK-8® solution was added to each well, and the sample mixtures were placed in a spectrophotometer (BioTek) to determine the absorbance at a wavelength of 450 nm. The percentage of viable cells was then calculated as follows:

$$\text{Cell viability } (\%) = OD_{sample} - OD_{blank}/OD_{control} - OD_{blank} \times 100 \quad (1)$$

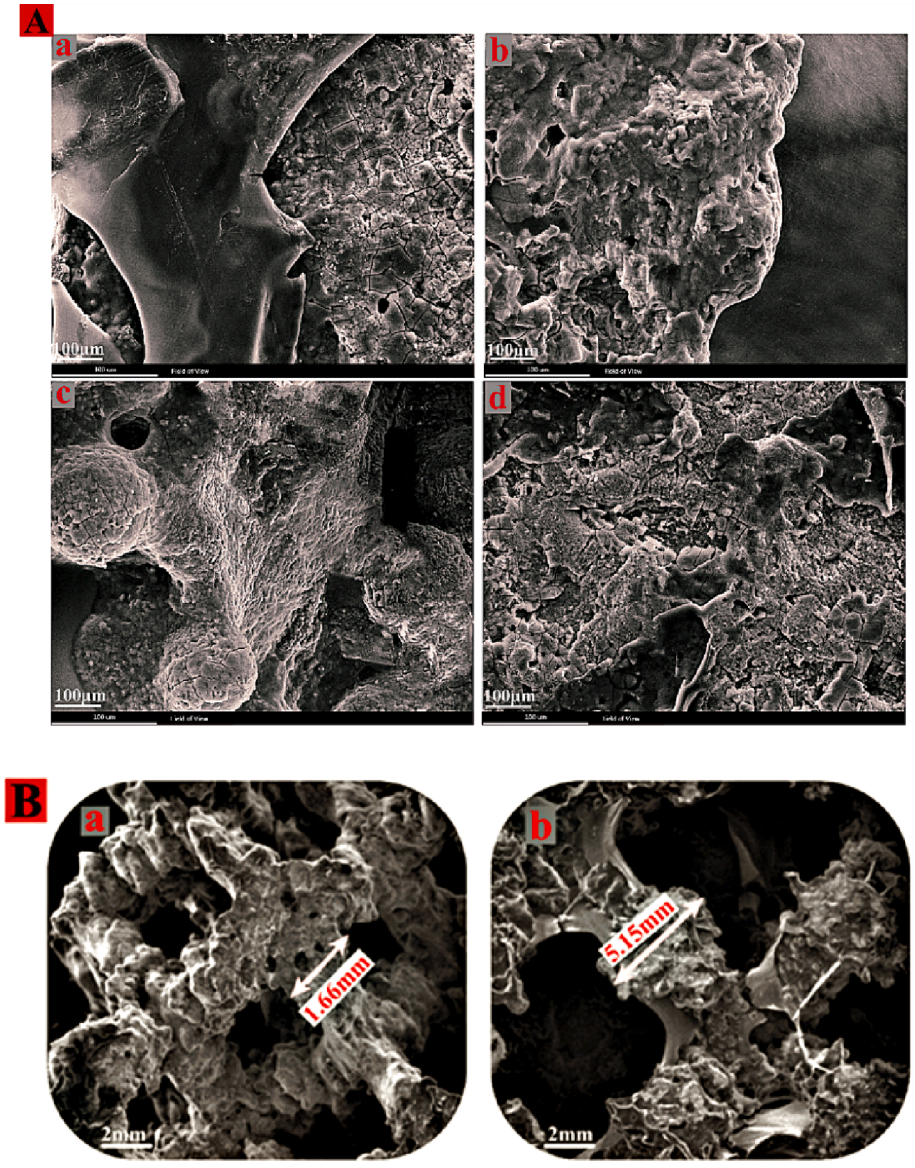

Fig. 2. (A) The SEM micrographs of surfaces (a) Mono [(Gel/Alg-IGF-1) Chi-Cef], (b) Multi [(Gel/Alg-IGF-1) Chi-Cef], (c) Mono [(4Gel/Alg-IGF-1) Chi-Cef], and (d) Multi [(4Gel/Alg-IGF-1) Chi-Cef]. (B) Surface porosities and coating thickness (a) Mono and (b) Multi polymeric carriers, respectively.

where the OD_{sample}, $OD_{control}$, and OD_{blank} are the optical densities of the sample, the control sample, and the blank well, respectively.

The porous samples were sterilized with 70 % ethanol for 10 min and employed directly for the cell adhesion assay. The osteoblast-like MG63 cell line was seeded at a density of 6000 cells per cm^2 in a cell culture medium and cultured for 7 days. The samples were washed with PBS and fixed with 4 % paraformaldehyde (PFA) for 20 min at room temperature. The samples were dehydrated in ascending ethanol concentrations (30, 50, 70, 80, 90, 96, and 100 %) for 10 min each. After drying in a ventilated hood and sputtering with gold, the samples were investigated using an SEM (Philips XL30, Netherlands).

2.6. Differentiation test

Human osteoblast-like MG-63 cells were cultured in DMEM (Gibco, USA) with 10 % fetal bovine serum (FBS), 1 % penicillin–streptomycin at 37 °C in 5 % CO_2 humidified atmosphere. The conditioned medium was prepared by soaking the scaffolds in cell culture medium without FBS for 24 h. The conditioned medium was collected and sterilized with 0.22 um filter. The cells were seeded into 96-well plates at a density of 10^4 cells/well and cultured in the conditioned medium for 3 days. The cells were cultured in osteoinductive medium including 100 nM dexamethasone (Sigma-Aldrich), 10 mM β-glycerophosphate (Sigma-Aldrich) and 50 μg/ml ascorbic acid (Sigma-Aldrich) for additional 14 days. The cells were washed with PBS and fixed with 4 % PFA for 20 min at room temperature. The cells were stained with alkaline phosphatase (Sigma-Aldrich) by following the supplier's instructions and observed using a microscope.

2.7. The antibacterial assay

2.7.1. Zone inhibition (ZOI)

The antibacterial activity of monolayer and multilayer carriers (Gel/Alg-IGF-1/Chi-Cef), (4Gel/Alg-IGF-1/Chi-Cef) on dode thin Ti64 bone scaffolds was tested against Gram-positive *S. aureus* (Staphylococcus aureus, ATCC 25923) bacteria obtained from the Pasteur Institute in Iran. The microorganisms were first developed in a saline buffer to optimize growth (10^6 CFU/ml) and then allowed to grow overnight in an incubator (35 ± 2 °C). The spread plate method was used to inoculate tryptone soy agar plates with a bacterial suspension of 1 ml for antimicrobial activity. Ti6Al4V Scaffold with carriers of cefazolin (Monolayer and Multilayer: (Gel/Alg-IGF-1) + Chi-Cef, (4Gel/Alg-IGF-1) + Chi-Cef, n = 3) were distributed onto the inoculated Petri dishes and then incubated at 37 °C overnight. The clear areas created around each carrier were measured and described as zones of inhibition (Rao et al., 2014). The greater the inhibitory zone diameter, the higher the level of antimicrobial activity.

2.7.2. Quantitative bacterial test

To evaluate the value of the antimicrobial activity of the specimens, the colony-forming units (CFU) were measured. The scaffolds were sterilized with ethanol for 10 min before the bacterial proliferation assay. They were then placed in a culture plate and covered with bacterial solutions (0.4 cc < V < 1 cc) for 1, 3, 6, and 24 h. All scaffolds were kept at 37 °C in an incubator containing 5 % CO_2. The control, as-built Ti6Al4V modified without the carrier, was added to the wells to confirm the incubation process. The suspension in each well was measured using a colony counter.

$$\text{CFU/ml} = (\text{no. of colonies} \times \text{dilution factor})/\text{volume of culture plate} \quad (2)$$

2.8. Release of drugs

The scaffolds from different groups were submerged in 5000 μl of PBS (pH = 7.2–7.4, 0.01 M) in a bain-marie at 37 °C. The PBS was refreshed on days 1, 7, and 14. The concentrations of IGF-1 and cefazolin in the samples at indicated time points were measured to determine drug release. The concentration of IGF-1 was measured using an ELISA kit for human IGF-1 (Abcam, ab100545), and the concentration of cefazolin was measured using ultra-performance liquid chromatography with UV detection (UPLC-UV). The mobile phase mixture consisted of 1.7 % formic acid with deionized water and 1 % formic acid in acetonitrile. The samples were eluted using a linear gradient elution program of 90 % water to 30 % acetonitrile at a flow rate of 1 ml/min at room temperature. The concentrations of cefazolin were measured by a UV/V detector at 270 nm after the defined time.

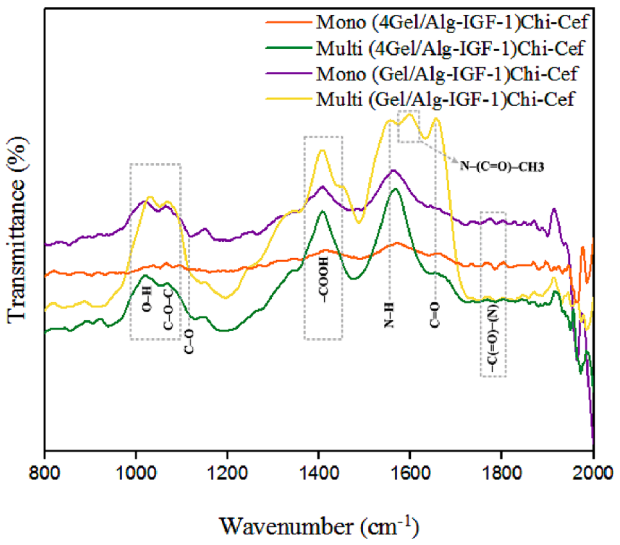

Fig. 3. FTIR analysis of the Ti64 scaffolds containing polymeric carriers.

2.9. Statistical analysis

The mean ± standard deviation was used to express all result data. Statistical calculations were analyzed using ANOVA to evaluate the differences among different groups. The experiment was considered significant when $p < .01$.

3. Result and Discussion

3.1. Surface characterization

Fig. 2A shows representative SEM images of mono and multi bilayers composed of IGF-1 and Cefazolin. The coatings consist of uniformly distributed polymeric layers that create a smooth surface. It was illustrated that the drug-releasing carriers are deposited in the walls and pores of porous structures without changing the scaffolds. Also, the porosity of the structures remained unobstructed (Fig. 2B), and the carrier covers the surface without filling the pores. However, the polymeric carrier created micro-cracks, as demonstrated by the evidence (Correlo et al., 2007; He and Liu, 2019). The presence of polymers may have increased water absorption, leading to the evaporation process and subsequent cracking. Fig. 2B shows that the minimum thickness of the lattice structure arm was observed on the monolayer surfaces (1.66 mm), whereas the multilayer carrier had a thickness of 5.15 mm. To verify that the drug-containing carrier formed through the interaction between polycation and polyanion (polyelectrolytes), the FTIR spectrum of additively manufactured scaffolds (as shown in Fig. 3) was measured. The deposition of drug-containing carriers onto bone scaffolds was achieved through specific interactions such as electrostatic, hydrogen or covalent bonds. The carrier (Gel/Alg-IGF-1) + Chi-Cef exhibited

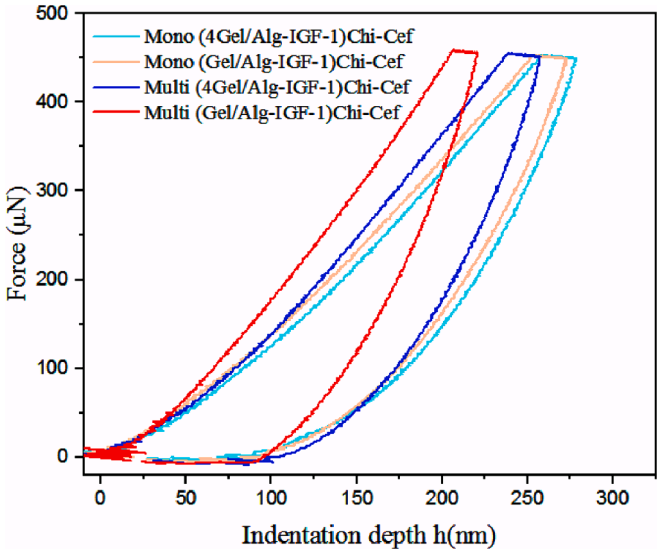

Fig. 4. Load/unload-displacement curve for the nanoindentation experiment.

Table 1
Experimental data derived from the nanoindentation test.

Type of carriers	Hardness (GPa)	Young Modulus (GPa)
Mono [(4Gel/Alg-IGF-1) Chi-Cef]	0.40	4.2
Mono [(Gel/Alg-IGF-1) Chi-Cef]	0.43	4.2
Multi [(4Gel/Alg-IGF-1) Chi-Cef]	0.45	5.2
Multi [(Gel/Alg-IGF-1) Chi-Cef]	0.64	6.8

characteristic stretching bands, including C = O stretching, N–H, and –COOH groups at 1634 cm^{-1}, 1539 cm^{-1}, and 1406 cm^{-1}, respectively. Additionally, characteristic peaks were observed at 1151 cm^{-1} (C–O), 1068 cm^{-1} (C–O–C), and 1020 cm^{-1} (O–H). The interaction may be attributed to the carboxyl ($–COO^-$) ions of the polyanions and the ammonium ($–NH_3^+$) ions of the polycation. In fact, the 1634 cm^{-1} band of carriers and the strengthened $–COO^-$ band at 1406 cm^{-1}, which is close to pure gelatin bands, indicate efficient bonding of gelatin. The interaction may be due to the conversion of electrostatic bonds into chemical bonds by hydrogen bonding between the gelatin $–COO^-$ ions and the chitosan $–NH_3^+$ ions (Lou et al., 2017; Zhang et al., 2022). The characteristic bands of chitosan were observed as overlapping peaks located at 1596 cm^{-1} (amide-II). The 1160 cm^{-1} amino peak of chitosan overlapped with the 1151 cm^{-1} peaks that corresponded to the interaction of alginate and chitosan through electrostatic forces (Li et al., 2005). Moreover, the emergence of amide-I peaks at 1796 cm^{-1} suggests a strong electrostatic interaction (Wang et al., 2017). It can be observed that the intensity of the bands decreased with decreasing bilayers in the monolayer samples.

3.2. Nanoindentation

Nanoindentation methodologies provide valuable insights into the mechanical properties of coatings on substrates (Shen, 2019), which depends on hardness and Young's modulus. Fig. 4 illustrates the load–displacement plots for different carrier structures, revealing distinct behaviors. It can be seen that the hardness increases with an increasing number of layers, particularly affecting the alginate component. This phenomenon arises from the layer-substrate interaction, influencing the measured hardness. The results indicate that monolayer and multilayer (4Gel/Alg-IGF-1) + Chi-Cef carriers exhibit a hardness of approximately 0.4 GPa, while the (Gel/Alg-IGF-1) + Chi-Cef multilayer demonstrates a hardness of approximately 0.6 GPa. Additionally, the load-unload curves reveal an elastic component across all carrier types.

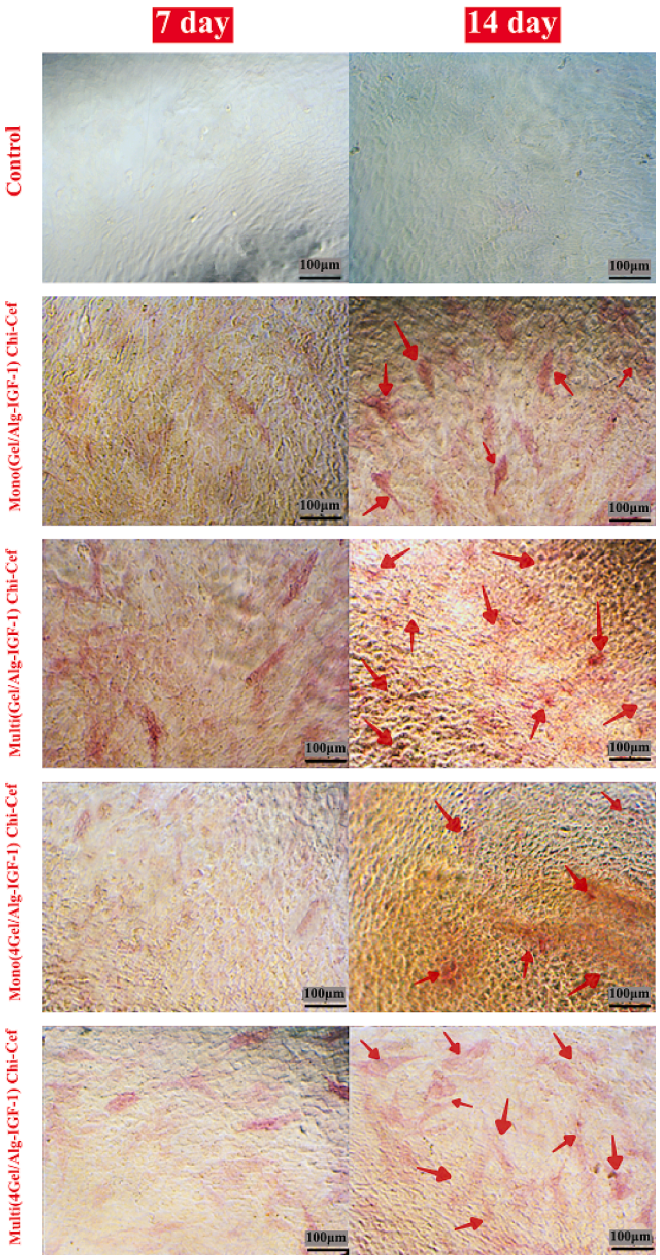

Fig. 5. The Effects of carriers containing IGF-1 and cefazolin on bone differentiation in MG63.

Interestingly, the depth value during unloading is significantly higher for monolayer carriers compared to their multilayer counterparts. Table 1 summarizes Young's modulus and hardness values obtained from our nanoindentation experiments.

3.3. Cell differentiation test

Alkaline phosphatase (ALP) is the most widely recognized biochemical marker for osteoblast differentiation. A previous study showed that ALP activity of MG63 cell occurs in a time-dependent manner and can be evaluated for up to 21 days during osteoblast differentiation (Zhou et al., 2019). Osteoblast-like cells were stained with alkaline phosphatase after 7 and 14 days of culture in the scaffold extract solution. The influence of IGF-1 on differentiation varied depending on the type of carriers and the phase of differentiation. Fig. 5 displays the distribution of red-quinone derivatives, which was utilized to assess differentiation and cell growth, as observed under an inverted optical

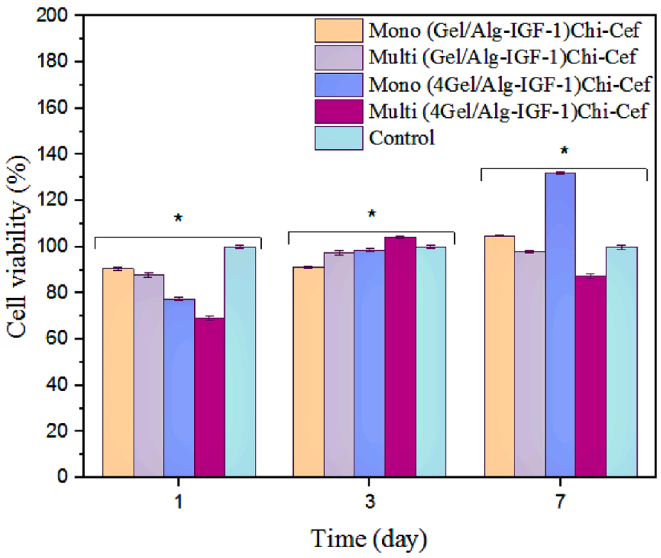

Fig. 6. WST colorimetric assay for cellular metabolic activity of carriers containing drugs.

microscope. The bright red region and the depth of redness represents enzyme activity. Multilayer carriers indicated more ALP activity on the ECM. During the 7-day culture period, cell differentiation was mostly higher in multi (Gel/Alg-IGF-1) + Chi-Cef and multi (4Gel/Alg-IGF-1) + Chi-Cef compared to the other groups. The degree of differentiation increased with the extension of the culture period and degree of differentiation. The study examined the effect of extract solutions with monolayer and multilayer carriers of IGF-1/Cef on cell culture. The results showed that after 14 days of incubation, the concentration of polymer in [(Gel/Alg-IGF-1) Chi-Cef] had the most significant effect on promoting MG63 cell growth. However, all carrier groups, particularly monolayers, provided less support for the early stage of osteogenic expression than the late stage. Four groups exhibited a similar tendency in terms of the expression levels of genes associated with to osteogenic differentiation. Several factors, such as the varying ratio of Gel/Alg and the mechanical properties of blend polymers (Begines et al., 2022), the differences in density between anionic polymers (Gel/Alg), and the IGF-1 dosage in monolayer and multilayer carriers (Amin Yavari et al., 2020), can impact the stability of growth factor release and compromise their effectiveness as carriers on porous Ti64. It is important to note that IGF-1 has a critical effective dosage range of 10.0–500 μg/l, which has been demonstrated to have beneficial effects on differentiation and safety (Locatelli and Bianchi, 2014). IGF-1 also affects intracellular signalling pathways related to osteogenic differentiation (ERK1/2), which may influence bone growth (Guntur and Rosen, 2013).

3.4. Biological Assays: WST test and cell morphology

Scaffolds were prepared using the LbL self-assembly method to create sustained polymeric carriers, including mono (Gel/Alg-IGF-1) + Chi-Cef, multi (Gel/Alg-IGF-1) + Chi-Cef, mono (4Gel/Alg-IGF-1) + Chi-Cef, and multi (4Gel/Alg-IGF-1) + Chi-Cef. The WST assay was used to determine cell proliferation and toxicity in extracts cultivated with MG63 cells for 1, 3, or 7 days. Fig. 6 compares of cell viability percentages for different groups over 7 days. Significant differences exist between each group. The outcomes demonstrate that different samples have varying levels of cell viability at the same time interval. As the incubation time increases, the cell count increases. Furthermore, the cell proliferation rate is displayed as mono (4Gel/Alg-IGF-1) + Chi-Cef > mono (Gel/Alg-IGF-1) + Chi-Cef > multi (Gel/Alg-IGF-1) + Chi-Cef > multi (4Gel/Alg-IGF-1) + Chi-Cef. Cell viability increased slightly in all samples over the course of three days. It is worth mentioning that multi (4Gel/Alg-IGF-1) + Chi-Cef has undergone significant changes. Interestingly, on the seventh day, the mono (4Gel/Alg-IGF-1) + Chi-Cef carriers exhibited higher viability than the other carriers. That is to say, the monolayer bilayer group had a more favorable influence on cell proliferation compared to the multilayer group. However, the joint functions of drug profiles and polymeric groups played an important role in promoting cell proliferation (Fortuni et al., 2019). Previous studies have shown that IGF-1 has a mitogenic influence at doses of approximately 10.0–500 μg/l after 3 days (Ni et al., 2013). After 7 days, cell viability exhibited a suitable trend of response to the increasing bilayer carriers.

The SEM examination revealed that the MG63 cells adhered, grew, and distributed throughout the surfaces of four distinct sample groups after 7 days. Additionally, the MG63 cells adhered strongly to the porous surface of the scaffolds. A comparison of the morphologies of MG63 cell surfaces on scaffolds after culture incubation time is presented below. According to Fig. 7(d), (b), it can be demonstrated that the cell count of groups multi (4Gel/Alg-IGF-1) + Chi-Cef and multi (Gel/Alg-IGF-1) +

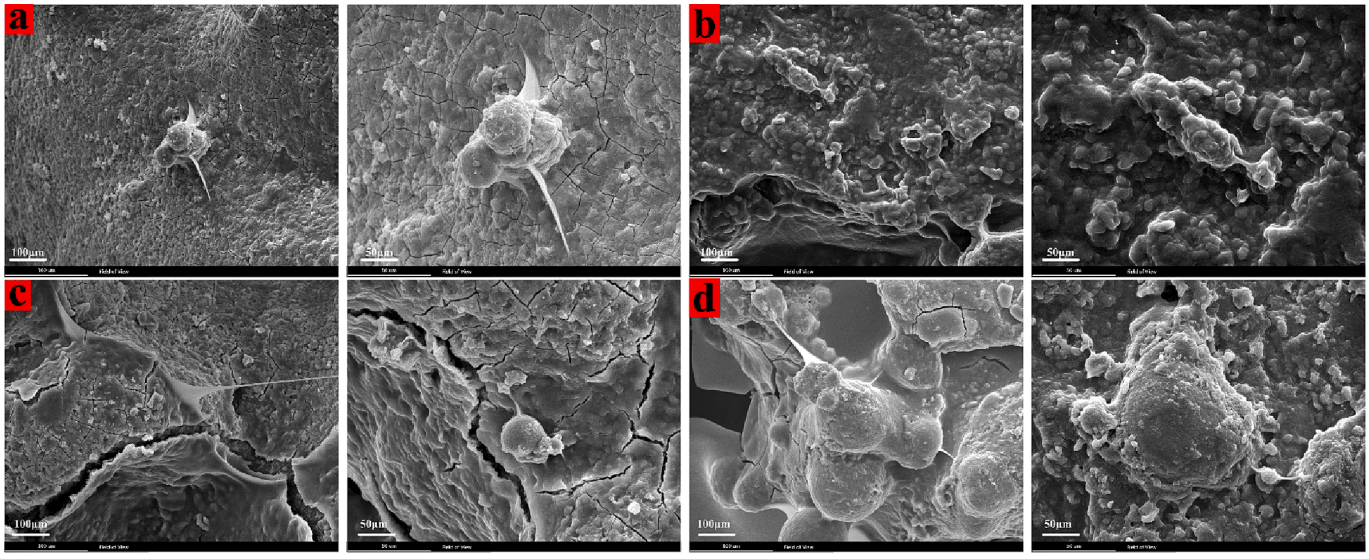

Fig. 7. Adhesion of MG63 cells to porous substrate containing drugs. (a) Mono [(Gel/Alg-IGF-1) Chi-Cef], (b) Multi [(Gel/Alg-IGF-1) Chi-Cef], (c) Mono [(4Gel/Alg-IGF-1) Chi-Cef], and (d) Multi [(4Gel/Alg-IGF-1) Chi-Cef].

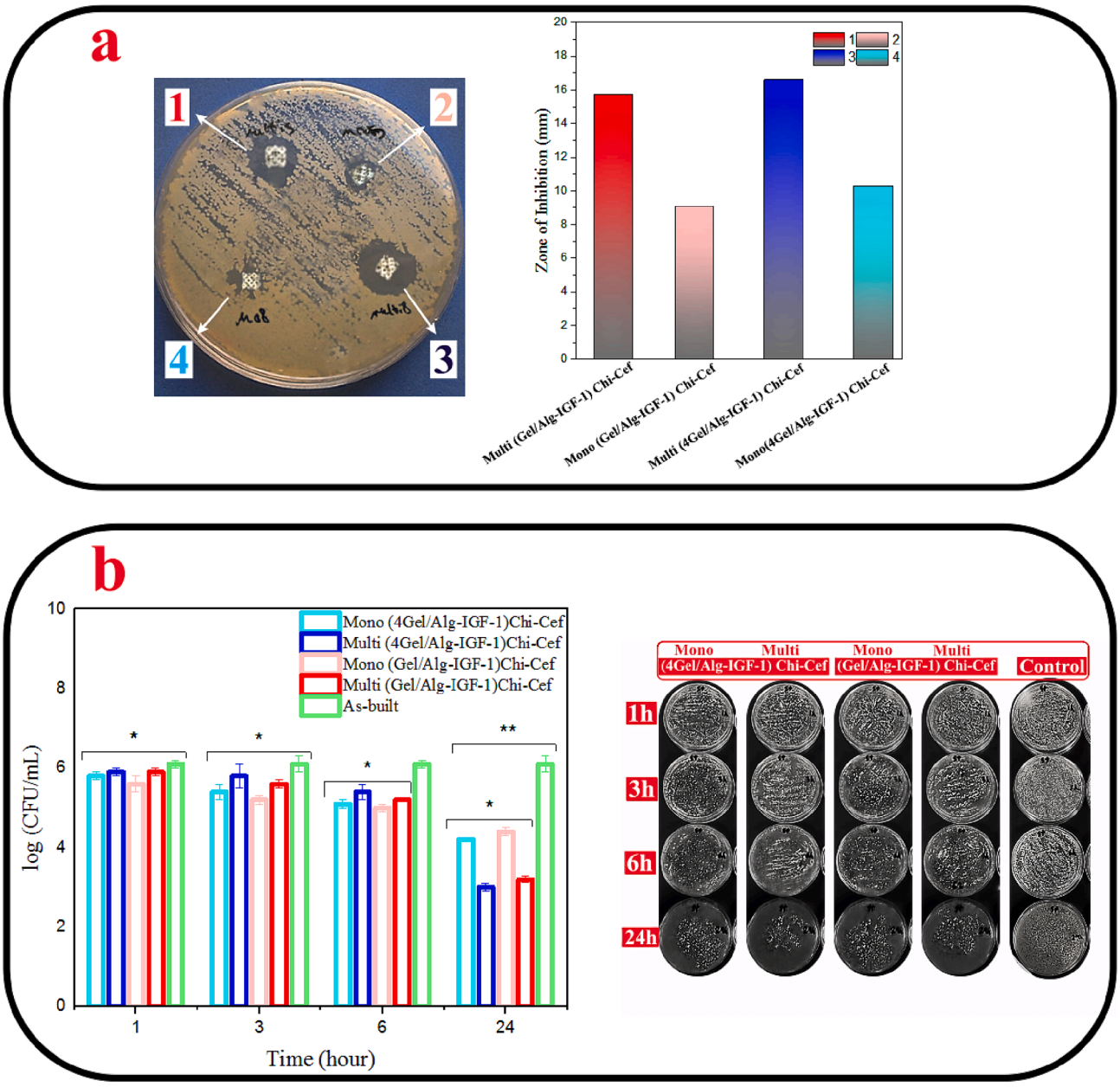

Fig. 8. Antibacterial activity of as-loaded carriers containing Cefazolin on Ti6Al4V scaffolds. (a) Zone of inhibition, (b) CFU (Colony forming unit) counts after exposure to carriers.

Chi-Cef on the scaffold's surface is significantly higher than that of the other groups. The surface of the scaffold is covered with irregularly shaped cells that have several filopodia extensions attached to them, and some of the cells have migrated through the pores. In addition, MG63 cells attached to the multi (Gel/Alg-IGF-1) + Chi-Cef scaffolds spread extensively with their filopodia adhered to the edge of pores, as shown in Fig. 7(b) (Guadarrama Bello et al., 2017). In contrast, comparatively less MG63 cells adhere to the scaffolds of mono (Gel/Alg-IGF-1) + Chi-Cef and mono (4Gel/Alg-IGF-1) + Chi-Cef than other groups. The cells on the surface of group mono (Gel/Alg-IGF-1) + Chi-Cef spread and had undeveloped filopodia, as displayed in Fig. 7(a). The cells on the scaffolds became irregular in shape after 7 days of culturing.

3.5. Antibacterial assay

The antimicrobial activity of Gel/Alginate-IGF-1/Chi-Cef carriers was measured against one important microorganism, Staphylococcus aureus (gram-positive). The well diffusion assay showed a significant enhancement in the zone of inhibition pattern with increased multilayer carriers containing drugs. The multilayer and monolayer carriers, (4Gel/Alg-IGF-1) + Chi-Cef and (Gel/Alg-IGF-1) + Chi-Cef, respectively, exhibited an inhibition zone against *S.aureus* with a maximum size of 16 ± 0.6 mm diameter and 15 ± 0.7 mm diameter, and a minimum size of 10 ± 0.3 mm diameter and 9 ± 0.1 mm diameter, respectively (Fig. 8a). Furthermore, the effect of drug-containing carriers on microorganism counts over time has been analyzed (Fig. 8b). The bacterial count of *S. aureus* strains in the scaffolds treated with antibiotics significantly decreased compared to the control group. These findings are consistent with the zone of inhibition test. However, it is worth noting that there was a substantial decrease in CFU in four cases compared to the control group after 24 h. The influence of carriers on the CFU of *S. aureus* was investigated. After 24 h, multilayer carriers showed significant drop in CFU than monolayer carriers. However, *S. aureus* exhibited similar behavior on (4Gel/Alg-IGF-1) + Chi-Cef and (Gel/Alg-IGF-1) + Chi-Cef

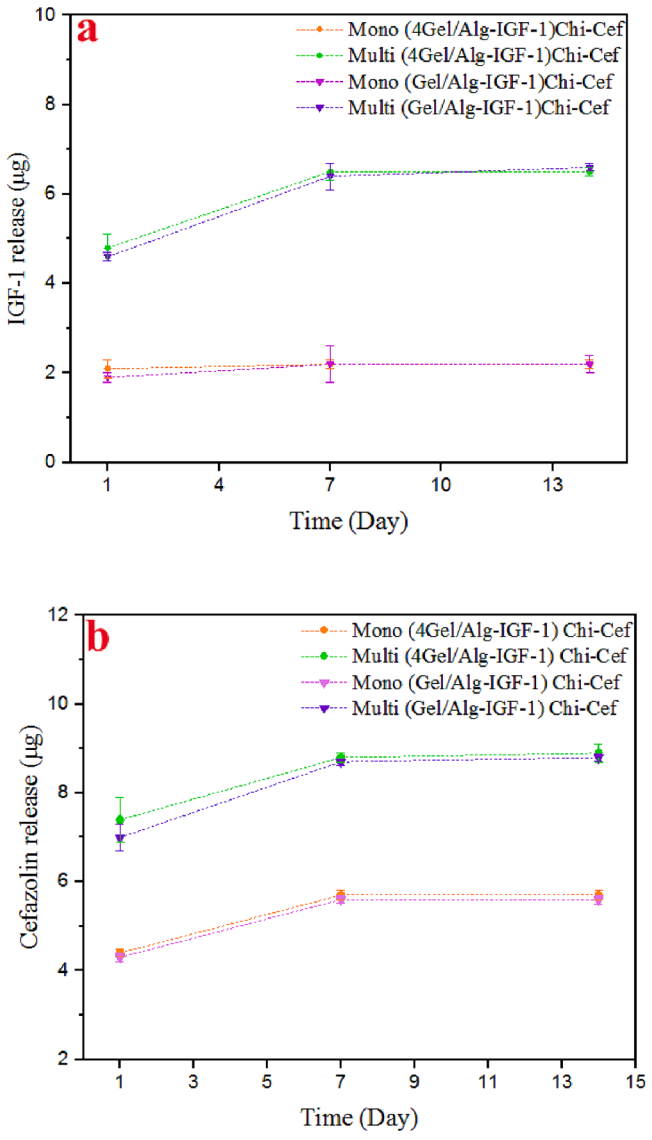

Fig. 9. Comparative release between monolayer and multilayer carriers, (a) IGF-1 growth factor release, and (b) Cefazolin antibiotic release.

monolayers. The bacterial reduction rate of multilayer carriers was mostly noticed, which was attributed to a higher loading dose of cefazolin (Proshin et al., 2022; Wang et al., 2004). Notably, the cefazolin has a minimum inhibitory concentration against pathogens (Zeller et al., 2009).

3.6. Drugs release

Self-assembly monolayer, and layer-by-layer assembly methods (Choi et al., 2017) are thin film strategies that enable the controlled release of active factors and drugs. Polyelectrolyte assemblies, such as monolayers and multilayer carriers, are primarily responsible for the storage and direct delivery of drugs (Guzmán et al., 2013). Generally, increasing the number of layers through the layer-by-layer process enhances the storage capacity in a multilayer carrier. The release of therapeutic agents is significantly influenced by the ratios of blend polymers (Nyamweya, 2021). The mechanical properties of the blend polymers were found to improve with an increased content of alginate (Begines et al., 2022). The percentage of alginate composition affects the dosage of the released drug. In all groups containing IGF-1 and Cefazolin, there was an initial release followed by an additional release (Fig. 9(a),(b)). The burst release was significant for all of the (Gel/Alg-IGF-1) + Chi-Cef carriers. However, the cumulative release of cefazolin from multilayers was higher than that from monolayers. The release of cefazolin from monolayer carriers was completed in less than 7 days. For instance, Wei et al. (Wei et al., 2013) synthesized a cefazolin/chitosan coating on a MAO film, and the release was almost complete before 7 days of immersion. Multilayer carriers indicate that quick release occurs after one day of immersion and sustained release for at least 10 days. This is attributed to the superior cefazolin content on the layers and thick antibiotic film. Compared with other polymeric carriers, (Gel/Alg-IGF-1) + Chi-Cef had a longer sustained release time. Previous studies (Shidfar et al., 2017) have shown that the total time of gentamicin/chitosan release from the coating can be controlled for approximately 10 days. The IGF-1 Cumulative (Fig. 9(a)) shows an initial release after 24 h of soaking, which increased with enhanced layers of carriers. Likewise, the multilayer carrier (4Gel/Alg-IGF-1) + Chi-Cef also demonstrated the highest initial release, due to a higher degradation rate compared to the carrier with a higher alginate amount (Gel/Alg-IGF-1) + Chi-Cef. It should be considered that the release of (Gel/Alg-IGF-1) + Chi-Cef was more sustained than that of (4Gel/Alg-IGF-1) + Chi-Cef carriers, and the release of IGF-1 was slower for the former (Fig. 9a). Yavari et al. (Amin Yavari et al., 2020) attempted to control the drug delivery rate of a coating containing BMP through LbL self-assembly.

4. Conclusion

In this investigation an attempt was made to apply Gel/Alg-Chi carriers containing IGF-1 and cefazolin onto the treated porous Ti64 surface using LbL self-assembly. The dual application of IGF-1 growth factor and cefazolin antibiotic enhances the adhesion, differentiation, and antibacterial properties of MG63 osteoblast-like cells, facilitated by the carriers. From this investigation, the following important conclusions are derived:

1) The LbL self-assembly provided a platform for encapsulating Ti64 porous surfaces independent of the polymeric ratio.
2) The number of bilayers, which includes both monolayer and multilayer carriers, exhibits a positive correlation with the proliferation and differentiation of MG63 cells. MG63 cells demonstrate optimal differentiation when treated with the combination of Insulin-like growth factor 1 (IGF-1) and cefazolin loaded onto the multilayered carrier (4Gel/Alg-IGF-1) + Chi-Cef. Also, the impact of polymeric concentration is clearly evident in the monolayer configuration (4Gel/Alg-IGF-1) + Chi-Cef.
3) Both mono- and multi-bilayer carriers demonstrated adequate and effective antimicrobial efficacy against S. aureus, achieved through controlled release of cefazolin, along with satisfactory biocompatibility in vitro.
4) The drug release increased during the first day for each scaffold, but after that, the IGF-1 was gradually or almost constantly released over a period of 14 days. The release rate was sustained by increasing the number of bilayers and reducing the gelatin ratio.
5) The release of cefazolin indicated that the concentration of multilayer carriers remained higher than that of monolayers for 7 days. Also, the concentration of multi (4Gel/Alg-IGF-1) + Chi-Cef stayed above that of the multi (Gel/Alg-IGF-1) + Chi-Cef.

CRediT authorship contribution statement

Parinaz Mofazali: Writing – review & editing, Writing – original draft, Visualization, Methodology, Investigation, Formal analysis, Data curation, Conceptualization. **Masoud Atapour:** Supervision, Methodology, Investigation, Formal analysis, Data curation, Conceptualization. **Miho Nakamura:** Methodology, Investigation, Funding acquisition. **Manuela Galati:** Methodology, Investigation, Funding acquisition.

Abdollah Saboori: Methodology, Investigation, Funding acquisition, Formal analysis.

Declaration of competing interest

The authors declare that they have no known competing financial interests or personal relationships that could have appeared to influence the work reported in this paper.

Data availability

The data that has been used is confidential.

Acknowledgements

This work was supported by the Iran National Science Foundation (INSF, No. 4006289). Also, the Integrated Additive Manufacturing centre at Politecnico di Torino (IAM@polito) is acknowledged for sample production.

References

Amin Yavari, S., Croes, M., Akhavan, B., Jahanmard, F., Eigenhuis, C.C., Dadbakhsh, S., Vogely, H.C., Bilek, M.M., Fluit, A.C., Boel, C.H.E., van der Wal, B.C.H., Vermonden, T., Weinans, H., Zadpoor, A.A., 2020. Layer by layer coating for bio-functionalization of additively manufactured meta-biomaterials. Addit. Manuf. 32, 100991 https://doi.org/10.1016/j.addma.2019.100991.

Aranaz, I., Alcántara, A.R., Civera, M.C., Arias, C., Elorza, B., Heras Caballero, A., Acosta, N., 2021. Chitosan: An overview of its properties and applications. Polymers (Basel). 13 https://doi.org/10.3390/polym13193256.

Arciola, C.R., Campoccia, D., Montanaro, L., 2018. Implant infections: adhesion, biofilm formation and immune evasion. Nat. Rev. Microbiol. 16, 397–409. https://doi.org/10.1038/s41579-018-0019-y.

Baughman, R., Zakhidov, A., Heer, W.A., 2002. Fuzzy nanoassemblies: Toward layered polymeric multicomposites. Science 80-, 297.

Begines, B., Arevalo, C., Romero, C., Hadzhieva, Z., Boccaccini, A.R., Torres, Y., 2022. Fabrication and characterization of bioactive gelatin–alginate–bioactive glass composite coatings on porous titanium substrates. ACS Appl. Mater. Interfaces 14, 15008–15020. https://doi.org/10.1021/acsami.2c01241.

Chen, X., Zhou, J., Qian, Y., Zhao, L., 2023. Antibacterial coatings on orthopedic implants. Mater. Today Bio 19, 100586. https://doi.org/10.1016/j.mtbio.2023.100586.

Choi, D., Park, J., Heo, J., Oh, T.I., Lee, E., Hong, J., 2017. Multifunctional collagen and hyaluronic acid multilayer films on live mesenchymal stem cells. ACS Appl. Mater. Interfaces 9, 12264–12271. https://doi.org/10.1021/acsami.7b00365.

Chua, P.-H., Neoh, K.-G., Kang, E.-T., Wang, W., 2008. Surface functionalization of titanium with hyaluronic acid/chitosan polyelectrolyte multilayers and RGD for promoting osteoblast functions and inhibiting bacterial adhesion. Biomaterials 29, 1412–1421. https://doi.org/10.1016/j.biomaterials.2007.12.019.

Correlo, V.M., Pinho, E.D., Pashkuleva, I., Bhattacharya, M., Neves, N.M., Reis, R.L., 2007. Water absorption and degradation characteristics of chitosan-based polyesters and hydroxyapatite composites. Macromol. Biosci. 7, 354–363. https://doi.org/10.1002/mabi.200600233.

Dallo, M., Patel, K., Hebert, A.A., 2023. Topical Antibiotic Treatment in Dermatology. Antibiot. (Basel, Switzerland) 12. doi: 10.3390/antibiotics12020188.

Donlan, R.M., Costerton, J., 2002. Biofilms: Survival mechanisms of clinically relevant microorganisms. Clin. Microbiol. Rev 15, 167–193.

Dunne, W., 2002. Bacterial adhesion: Seen any good biofilms lately? Clin. Microbiol. Rev 15, 155–166.

Eady, E.A., Cove, J.H., 1990. Topical antibiotic therapy: current status and future prospects. Drugs Exp. Clin. Res. 16, 423–433.

Engesaeter, L.B., Lie, S.A., Espehaug, B., Furnes, O., Vollset, S.E., Havelin, L.I., 2003. Antibiotic prophylaxis in total hip arthroplasty: effects of antibiotic prophylaxis systemically and in bone cement on the revision rate of 22,170 primary hip replacements followed 0–14 years in the Norwegian Arthroplasty Register. Acta Orthop. Scand. 74, 644–651. https://doi.org/10.1080/00016470310018135.

Fortuni, B., Inose, T., Ricci, M., Fujita, Y., Van Zundert, I., Masuhara, A., Fron, E., Mizuno, H., Latterini, L., Rocha, S., Uji-i, H., 2019. Polymeric Engineering of Nanoparticles for Highly Efficient Multifunctional Drug Delivery Systems. Sci. Rep. 9, 1–13. https://doi.org/10.1038/s41598-019-39107-3.

Fosca, M., Rau, J.V., Uskoković, V., 2022. Factors influencing the drug release from calcium phosphate cements. Bioact. Mater. 7, 341–363. https://doi.org/10.1016/j.bioactmat.2021.05.032.

Gallo, J., Holinka, M., Moucha, C.S., 2014. Antibacterial Surface Treatment for Orthopaedic Implants. Int. J. Mol. Sci. https://doi.org/10.3390/ijms150813849.

Guadarrama Bello, D., Fouillen, A., Badia, A., Nanci, A., 2017. A nanoporous titanium surface promotes the maturation of focal adhesions and formation of filopodia with distinctive nanoscale protrusions by osteogenic cells. Acta Biomater. 60, 339–349. https://doi.org/10.1016/j.actbio.2017.07.022.

Guntur, A.R., Rosen, C.J., 2013. IGF-1 regulation of key signaling pathways in bone. Bonekey Rep. 2, 437. https://doi.org/10.1038/bonekey.2013.171.

Guzmán, E., Ruano, M., Rubio, R.G., Ortega, F., 2013. Polyelectrolyte assemblies for drug storage and delivery: Multilayers, nanocapsules and multicapsules, Inhaler Devices: Fundamentals, Design and Drug Delivery. doi: 10.1533/9780857098696.2.94.

Harris, L.G., Richards, R.G., 2006. Staphylococci and implant surfaces: a review. Injury 37 (Suppl 2), S3–S. https://doi.org/10.1016/j.injury.2006.04.003.

He, G., Liu, Y., 2019. Theoretical modeling of the mechanical degradation of polymer composites due to moisture/water absorption and damage progression, in: AeroTech Americas. SAE Int. doi: 10.4271/2019-01-1376.

Ishiyama, M., Miyazono, Y., Sasamoto, K., Ohkura, Y., Ueno, K., 1997. A highly water-soluble disulfonated tetrazolium salt as a chromogenic indicator for NADH as well as cell viability. Talanta 44, 1299–1305. https://doi.org/10.1016/S0039-9140(97)00017-9.

Jiménez-Gómez, C.P., Cecilia, J.A., 2020. Chitosan: a natural biopolymer with a wide and varied range of applications. Molecules 25. https://doi.org/10.3390/molecules25173981.

Kjalarsdóttir, L., Dýrfjörd, A., Dagbjartsson, A., Laxdal, E.H., Örlygsson, G., Gíslason, J., Einarsson, J.M., Ng, C.-H., Jónsson, H.J., 2019. Bone remodeling effect of a chitosan and calcium phosphate-based composite. Regen. Biomater. 6, 241–247. https://doi.org/10.1093/rb/rbz009.

Kovačević, D., Pratnekar, R., Godič Torkar, K., Salopek, J., Dražić, G., Abram, A., Bohinc, K., 2016. Influence of Polyelectrolyte Multilayer Properties on Bacterial Adhesion Capacity. Polymers (basel). 8 https://doi.org/10.3390/polym8100345.

Li, W., Lei, X., Feng, H., Li, B., Kong, J., Xing, M., 2022. Layer-by-layer cell encapsulation for drug delivery: the history, technique basis, and applications. Pharmaceutics 14. https://doi.org/10.3390/pharmaceutics14020297.

Li, Z., Ramay, H.R., Hauch, K.D., Xiao, D., Zhang, M., 2005. Chitosan-alginate hybrid scaffolds for bone tissue engineering. Biomaterials 26, 3919–3928. https://doi.org/10.1016/j.biomaterials.2004.09.062.

Locatelli, V., Bianchi, V.E., 2014. Effect of GH/IGF-1 on bone metabolism and osteoporsosis. Int. J. Endocrinol. 2014, 235060 https://doi.org/10.1155/2014/235060.

Lou, T., Wang, X., Song, G., Cui, G., 2017. Synthesis and flocculation performance of a chitosan-acrylamide-fulvic acid ternary copolymer. Carbohydr. Polym. 170, 182–189. https://doi.org/10.1016/j.carbpol.2017.04.069.

Matabola, K.P., Bambo, M.F., Sikhwivhilu, K., Vatsha, B., Moutloali, R.M., 2015. Chemical Grafting of Polystyrene Sodium Sulfonate (PSS) onto Polyethersulfone (PES) Powder and Effect on the Characteristics of the Resultant Ultrafiltration Membranes. Mater. Today Proc. 2, 3957–3963. https://doi.org/10.1016/j.matpr.2015.08.025.

Mathews, S., Gupta, P.K., Bhonde, R., Totey, S., 2011. Chitosan enhances mineralization during osteoblast differentiation of human bone marrow-derived mesenchymal stem cells, by upregulating the associated genes. Cell Prolif. 44, 537–549. https://doi.org/10.1111/j.1365-2184.2011.00788.x.

Min, J., Choi, K.Y., Dreaden, E.C., Padera, R.F., Braatz, R.D., Spector, M., Hammond, P. T., 2016. Designer Dual Therapy Nanolayered Implant Coatings Eradicate Biofilms and Accelerate Bone Tissue Repair. ACS Nano 10, 4441–4450. https://doi.org/10.1021/acsnano.6b00087.

Mofazali, P., Atapour, M., Nakamura, M., Sheikholeslam, M., Galati, M., Saboori, A., 2024. Surface modification of additive manufactured Ti6Al4V scaffolds with gelatin/alginate- IGF-1 carrier: An effective approach for healing bone defects. Int. J. Biol. Macromol. 131125 https://doi.org/10.1016/j.ijbiomac.2024.131125.

Moris, T., Ehud, C., Lorin, S.A., Aviram, H., Avraham, S., Itamar, A., Mark, K., Narin-Nard, C., Guy, T., Yoram, O., Gilad, M., Eyal, N., Roy, B., Michael, G., Anna, M., Anat, M., Michal, D., Shmuel, B., Raphael, R., Sami, V., 2023. Regional Antibiotic Delivery for Implanted Cardiovascular Electronic Device Infections. J. Am. Coll. Cardiol. 81, 119–133. https://doi.org/10.1016/j.jacc.2022.10.022.

Ni, F., Sun, R., Fu, B., Wang, F., Guo, C., Tian, Z., Wei, H., 2013. IGF-1 promotes the development and cytotoxic activity of human NK cells. Nat. Commun. 4, 1479. https://doi.org/10.1038/ncomms2484.

Nyamweya, N.N., 2021. Applications of polymer blends in drug delivery. Futur. J. Pharm. Sci. 7 https://doi.org/10.1186/s43094-020-00167-2.

Oliva, A., Miele, M.C., Al Ismail, D., Di Timoteo, F., De Angelis, M., Rosa, L., Cutone, A., Venditti, M., Mascellino, M.T., Valenti, P., Mastroianni, C.M., 2021. Challenges in the microbiological diagnosis of implant-associated infections: a summary of the current knowledge. Front. Microbiol. 12 https://doi.org/10.3389/fmicb.2021.750460.

Oliveira, W.F., et al., 2018. Staphylococcus aureus and Staphylococcus epidermidis infections on implants. J. Hosp. Infect. 98, 111–117.

Oliver, W.C., Pharr, G.M., 1992. An improved technique for determining hardness and elastic modulus using load and displacement sensing indentation experiments. J. Mater. Res. 7, 1564–1583. https://doi.org/10.1557/JMR.1992.1564.

Pina, S., Ribeiro, V.P., Marques, C.F., Maia, F.R., Silva, T.H., Reis, R.L., Oliveira, J.M., 2019. Scaffolding strategies for tissue engineering and regenerative medicine applications. Materials (basel). 12, 1824.

Proshin, P.I., Abdurashitov, A.S., Sindeeva, O.A., Ivanova, A.A., Sukhorukov, G.B., 2022. Additive manufacturing of drug-eluting multilayer biodegradable films. Polymers (basel). 14 https://doi.org/10.3390/polym14204318.

Rao, P.J., Pelletier, M.H., Walsh, W.R., Mobbs, R.J., 2014. Spine interbody implants: material selection and modification, functionalization and bioactivation of surfaces to improve osseointegration. Orthop. Surg. 6, 81–89. https://doi.org/10.1111/os.12098.

Roca-Millan, E., Estrugo-Devesa, A., Merlos, A., Jané-Salas, E., Vinuesa, T., López-López, J., 2021. Systemic Antibiotic Prophylaxis to Reduce Early Implant Failure: A

Systematic Review and Meta-Analysis. Antibiot. (Basel, Switzerland) 10. doi: 10.3390/antibiotics10060698.
Shen, Y.-L., 2019. Nanoindentation for Testing Material Properties BT - Handbook of Mechanics of Materials, in: Schmauder, S., Chen, C.-S., Chawla, K.K., Chawla, N., Chen, W., Kagawa, Y. (Eds.), . Springer Singapore, Singapore, pp. 1981–2012. doi: 10.1007/978-981-10-6884-3_46.
Shidfar, S., Tavangarian, F., Nemati, N.H., Fahami, A., 2017. Drug delivery behavior of titania nanotube arrays coated with chitosan polymer. Mater. Discov. 8, 9–17. https://doi.org/10.1016/j.md.2017.09.002.
Stigter, M., de Groot, K., Layrolle, P., 2002. Incorporation of tobramycin into biomimetic hydroxyapatite coating on titanium. Biomaterials 23, 4143–4153. https://doi.org/10.1016/S0142-9612(02)00157-6.
Wall, V., Nguyen, T.-H., Nguyen, N., Tran, P.A., 2021. Controlling Antibiotic Release from Polymethylmethacrylate Bone Cement. Biomedicines 9. https://doi.org/10.3390/biomedicines9010026.
Wang, G., Liu, S.-J., Ueng, S.-W.-N., Chan, E.-C., 2004. The release of cefazolin and gentamicin from biodegradable PLA/PGA beads. Int. J. Pharm. 273, 203–212. https://doi.org/10.1016/j.ijpharm.2004.01.010.
Wang, G., Wang, X., Huang, L., 2017. Feasibility of chitosan-alginate (Chi-Alg) hydrogel used as scaffold for neural tissue engineering: a pilot study in vitro. Biotechnol. Biotechnol. Equip. 31, 766–773. https://doi.org/10.1080/13102818.2017.1332493.
Wei, D., Zhou, R., cheng, S., Feng, W., Li, B., Wang, Y., Jia, D., Zhou, Y., Guo, H., 2013. Microarc oxidized TiO2 based ceramic coatings combined with cefazolin sodium/chitosan composited drug film on porous titanium for biomedical applications. Mater. Sci. Eng. C 33, 4118–4125. doi: doi: 10.1016/j.msec.2013.05.053.
Xiao, F.-X., Pagliaro, M., Xu, Y.-J., Liu, B., 2016. Layer-by-layer assembly of versatile nanoarchitectures with diverse dimensionality: a new perspective for rational construction of multilayer assemblies. Chem. Soc. Rev. 45, 3088–3121. https://doi.org/10.1039/C5CS00781J.
Yu, Q., Wu, Z., Chen, H., 2015. Dual-function antibacterial surfaces for biomedical applications. Acta Biomater. 16, 1–13. https://doi.org/10.1016/j.actbio.2015.01.018.
Zeller, V., Durand, F., Kitzis, M.D., Lhotellier, L., Ziza, J.M., Mamoudy, P., Desplaces, N., 2009. Ctontinuous cefazolin infusion to treat bone and joint infections: Clinical efficacy, feasibility, safety, and serum and bone concentrations. Antimicrob. Agents Chemother. 53, 883–887. https://doi.org/10.1128/AAC.00389-08.
Zhang, J., Zhao, X., Kong, Q., Wang, X., Lou, T., 2022. Preparation of chitosan/DADMAC/lignin terpolymer and its application of dye wastewater flocculation. Polym. Bull. 79, 7479–7490. https://doi.org/10.1007/s00289-021-03863-y.
Zhou, H., Jiao, G., Dong, M., Chi, H., Wang, H., Wu, W., Liu, H., Ren, S., Kong, M., Li, C., Zhang, L., Chen, Y., 2019. Orthosilicic Acid Accelerates Bone Formation in Human Osteoblast-Like Cells Through the PI3K–Akt–mTOR Pathway. Biol. Trace Elem. Res. 190, 327–335. https://doi.org/10.1007/s12011-018-1574-9.
Ziminska, M., Dunne, N., Hamilton, A.R., 2016. Porous materials with tunable structure and mechanical properties via templated layer-by-layer assembly. ACS Appl. Mater. Interfaces 8, 21968–21973. https://doi.org/10.1021/acsami.6b07806.